FACILE ONE POT SYNTHESIS OF HIGHLY STABLE L-ASCORBIC ACID COATED MAGNETITE NANOPARTICLES DISPERSION

X. H. YAU[a], K. Y. YEW[b], C. S. KHE[a*], S. RAJALINGAM[a], C. W. LAI[c], W. W. LIU[d]

[a]*Department of Fundamental and Applied Sciences, Universiti Teknologi PETRONAS, 32610 Seri Iskandar, Perak, Malaysia*
[b]*Department of Petroleum Engineering, Universiti Teknologi PETRONAS, Bandar Seri Iskandar, 32610 Seri Iskandar, Perak, Malaysia*
[c]*Nanotechnology& Catalysis Research Centre (NANOCAT), Institute of Postgraduate Studies (IPS), University of Malaya, 3rd Floor, Block A, 50603 Kuala Lumpur, Malaysia*
[d]*Institute of Nano Electronic Engineering, University Malaysia Perlis, 01000 Kangar, Perlis, Malaysia*

Magnetite nanoparticles had been synthesized through a simple one pot and ecofriendly method. Biocompatible and nontoxic L-ascorbic acid (LAA) was used as capping agent in the synthesis process to produce highly stable magnetite nanoparticle dispersion. The magnetite nanoparticles were characterized with various techniques. From X-ray diffraction (XRD) and energy dispersive X-ray spectroscopy (EDX) analysis, the results reveal that magnetite nanoparticles were synthesized without impurities. Spherical magnetite nanoparticles with average particle size of 11.1 nm coated with LAA was shown in both scanning electron microscope (SEM) and transmission electron microscope (TEM) images. Fourier transform infrared spectroscopy (FTIR) and X-ray photoelectron spectroscopy (XPS) confirmed the LAA capped on the surface of magnetite nanoparticles, whereas Zeta potential shows the LAA coated magnetite nanoparticles were exhibit high stability with good dispersion. From vibrating sample magnetometer (VSM), the superparamagnetism of magnetite nanoparticles was confirmed. Possible mechanism of LAA capped on magnetite nanoparticles was proposed eventually.

1. Introduction

Metal nanoparticles are being studied extensively by the nanotechnology researchers in recent years due to their unique physical and chemical properties, such as, catalytic, electrical, optical, mechanical and magnetic properties [1-3]. Metal nanoparticles are widely applied in many engineering areas such as absorbents, biological and chemical sensors, catalysis, magnetic storage media and optoelectronics [4-9]. Magnetite (Fe_3O_4) nanoparticle is an example of metal nanoparticle with cubic inverse spinel structure and exhibit unique magnetic and electric properties which are attributed to the electrons transfer between Fe^{2+} and Fe^{3+} in the octahedral site [10,11]. It is also has the characteristic of good biocompatibility and low cytotoxicity. Thus, it attracted numerous attentions from researchers and many applications related to it have been explored. For instance, catalysis, magnetic sensing, color removal and some medical areas such as targeted drug carrier, radiofrequency hyperthermia, magnetic resonance imaging (MRI), magneto-optics devices and so on [12,13].

---

*Corresponding author: chengseong.khe@utp.edu.my

Various methods of synthesizing magnetite nanoparticles have been established such as hydrothermal synthesis, sonochemical synthesis, reverse micelles, thermal decomposition, microemulsion, wet chemical reduction and electrochemical techniques [12-15]. All these methods are eco-hazardous due to the application of toxic chemicals and energy intensive routes [16]. Thus, green chemistry is need in hour in order to develop an environment friendly method for synthesizing metal nanoparticles.

Green chemistry is the design, manufacture and applications of chemical products by strictly following the principles that reduces or eliminates the use and generation of hazardous substances and to restore the environment [17]. The twelve principles of green chemistry must be comprehensively addressed in the design of synthetic routes, chemical analyses, or chemical processes in order to sustain the environment [18]. There are three key factors in the synthesizing of metal nanoparticles following the concept of green chemistry which are the use of eco-friendly solvents, toxic free chemicals and renewable materials [19]. In reference to this principle, the eco-friendly surfactant has inspired the researchers in the field of synthesizing nanoparticles.

Generally, there are two types of classification of surfactant had been reported in the synthesis of magnetite nanoparticles which are natural ones (for instance, dextran, starch, lipids, glucose, chitosan, gelatin, etc.) and synthetic ones (polyvinyl alcohol (PVA), polyethylene glycol (PEG), etc.) [20]. All these surfactant possess its own advantages in synthesis of magnetite nanoparticles, but in spite of biocompatibility, they are not preferable for in vivo applications as aggregation does occur once the surfactant detach from the surface of nanoparticles [21].

The most important aspects in synthesizing the magnetite nanoparticles for utilization in various fields are the uniformity in size and shape distribution, colloidal stability, hydrophilicity or hydrophobicity of surfactant, magnetic properties and biocompatibility of the synthesized nanoparticles [22]. Thus, L-ascorbic acid (LAA) is suggested as surfactant in this work. LAA is one form of vitamin C which is a six carbon lactone produced by plants and some animal species [23]. LAA has been used in multiple applications, such as antioxidant, cosmetic and pharmaceutical, assay for erythrocyte hemolysis, food additives and production of graphene oxide sheets [24-26].

Thus far, there are only two research groups had been synthesizing magnetite nanoparticles using LAA. Feng and his co-workers have evaluated the ascorbic acid-coated magnetite nanoparticles which synthesized through hydrothermal approach as an absorbent to remove heavy metal arsenic from wastewater, whereas Sreeja's research group have synthesized water-dispersible ascorbic-acid-coated magnetite nanoparticles through reverse co-precipitation method that can acted as anti-oxidizing agent for contrast enhancement in MRI [21,27]. Hence, there is still lack of enough researches to evaluate its novel properties.

In this work, we are using a simple one pot synthesis, a more environmental friendly method to prepare magnetite nanoparticles which are coated with LAA and concurrently to access its novel properties when this modified approach was applied. In the experiments, different concentrations of LAA were applied and all reactions occurred in an aqueous medium. The magnetite nanoparticles obtained were characterized with various techniques and the results were discussed systematically. The possible mechanism of LAA coated on magnetite nanoparticles are briefly proposed eventually.

2. Experimental section

2.1. Materials

Iron(II) sulphate ($FeSO_4.7H_2O$), iron(III) chloride ($FeCl_3.6H_2O$), ammonium hydroxide (NH_4OH), ethanol and LAA were purchased from Merck. All the chemicals were used as received without further purification. Deionized water was used in all experiments.

2.2. Preparation of Magnetite Nanoparticles

In a typical reaction mixture, 2.78 g of iron(II) sulphate was added into 175 ml of deionized water in a 500ml beaker and followed by 3.25 g of iron(III) chloride. The solution became brownish. The mixture was heated to 80˚C under vigorously stirring condition using magnetic stirrer on hot plate until no solid particles were observed. After 15 to 20 minutes, once the solution's temperature was reached 80˚C, 15 ml of ammonium hydroxide was added rapidly into the beaker. The solution turned black immediately. The resulting suspension was stirred

vigorously for another 10 minutes. Then, LAA of different weight (0.24g, 0.48g, 0.72g, 0.96g) was added to the solution and maintained for another 60 minutes. These samples were labelled as FE2A0.24, FE2A0.48, FE2A0.72 and FE2A0.96 respectively. A control sample without addition of surfactant was designated as FE20. After that, the solution was left cool at room temperature. After cooling, the beaker was placed on top of a magnetic bar in order to separate the black particles from water. The black slurry was then collected, washed and dried in oven at 50˚C for 12 hours.

2.3. Characterization

X-ray diffraction (XRD) was performed using Bruker D8 advance diffractometer with CuKα radiation. Surface morphology was studied using ZEISS Leo Supra 55 variable pressure field emission scanning electron microscope (FESEM). The size and morphology of the samples were analyzed by using Philips CM12 transmission electron microscopy (TEM) with the acceleration voltage of 100kV. The surface bonding of the particles was recorded with Perkin Elmer Spectrum BX Fourier transform infrared spectroscopy (FTIR) in the range of 400-4000cm^{-1} using KBr pellet method. The X-ray photoelectron spectrum (XPS) was measured using Thermo Scientific K-Alpha instrument with Al Kα as the radiation source. The surface charge of nanoparticles was determined using Zetasizer Nano ZSP (Malvern instrument, UK) with a laser source of 633nm. Vibration sample magnetometer (DMS model 10) was used to examine the magnetic properties of the samples under magnetic fields up to 20 kOe.

3. Results and discussion

The structural characterization of samples was carried out by using X-ray diffraction (XRD) analysis within the angular range of $20^{o} \leq 2\theta \leq 90^{o}$. Figure 1a and 1b show the XRD patterns of magnetite nanoparticles synthesized at different temperatures without coating of surfactant. Meanwhile, figure 1c and 1d present the magnetite nanoparticles coated with different concentration of LAA. All samples showed in figure 1(a-d) had the same characteristic peaks which are located at 30.20˚, 35.52˚, 43.33˚, 53.71˚, 57.22˚ and 62.95˚ were corresponding to the (220), (311), (400), (422), (511) and (440) crystal planes of a pure Fe_3O_4 with a spinel structure (JCPDS file PDF no.65-3107) [28]. No impurities were detected in all samples as no extra diffraction peak was found. From figure 1a and 1b, it can be observed that the intensities of the peaks increased and the broadness of the peaks decreased as the synthesis temperature increased from 60˚C to 80˚C. The crystallite sizes of magnetite nanoparticles were determined using Debye-Scherrer formula[11]. The crystallite size of magnetite nanoparticles without surfactant coating at temperature of 60˚C and 80˚C were 6.55 nm and 12.84 nm, respectively. Thus, the increases in reaction temperature eventually increase the crystallite size of nanoparticles. This indicated the temperature play a crucial role in the particle growth [29]. Besides, the broad diffraction peaks obtained indicating that the small crystallite sized of nanoparticles produced [30].

Figure 1c and figure 1d show the XRD patterns of magnetite nanoparticles synthesized with different concentrations of LAA at same temperature i.e. 80°C. The average crystallite sizes for both samples were quite close to each other which are about 9 nm. This result indicated that different in LAA concentration had no much effect on the particle growth [31]. However, the presence of LAA surfactant in synthesis of magnetite nanoparticles had improved the crystallite size of nanoparticles. At 80°C, the average crystallite sizes of magnetite nanoparticles without and with LAA coating were 12.84 nm and 9 nm respectively. Smaller crystallite size of magnetite nanoparticles was obtained for the coated LAA magnetite nanoparticles because LAA stabilized the magnetite core and prevents the agglomeration of nanoparticles [20].
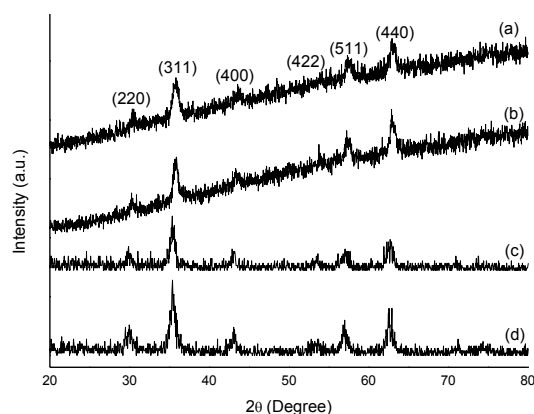
Fig. 1. XRD for the samples synthesized (a) without surfactant, 60°C, (b) without surfactant, 80°C, (c) with LAA, FE2A0.24 and (d) with LAA, FE2A0.96

The prepared magnetite nanoparticles were examined by using scanning electron microscopy (SEM) equipped with energy dispersive X-ray spectroscopy (EDX) in order to have a better understanding on the surface morphology and the atomic percentage of different elements of the synthesized nanoparticles. Figure 2a and 2b shows the SEM and EDX of samples which synthesized using LAA as surfactant, whereas figure 2c and 2d were for the samples synthesized without surfactant. In general, both SEM images for figure 2a and 2c shows the clear image of magnetite nanoparticles which are in spherical shape. The iron oxide nanoparticles in the cluster form were observed in figure 2c (nanoparticle synthesized without surfactant) which is due to the nature of magnetite nanoparticles. Magnetite nanoparticles were small in size, thus have large ratio of surface area over volume and contributed to high surface energy. Besides, the existence of attractive magnetic force also contributed to the unstable condition of magnetite nanoparticles. Thus, the magnetite nanoparticles without surfactant as capping agent were favor to agglomerate and form a large cluster in order to minimize the surface energies [20]. In contrast, figure 2a shows well dispersed magnetite nanoparticles as the LAA acted as both capping agent and stabilizer.

In general, both EDX in figure 2b and 2d contain the intense peaks of Fe and O. The composition of iron and oxygen elements is about 39.86% and 60.14% for magnetite nanoparticles synthesized with LAA surfactant as shown in figure 2b. On the other hand, the atomic percentages for the magnetite nanoparticles synthesized without surfactant (figure 2d) were 40.92% of Fe and 59.08% of O. The Fe and O signals were attributed to Fe_3O_4, this implies that the iron oxide nanoparticles were formed without impurities [32]. Besides, the atomic percentages value that obtained by EDX quantification could be used for reflecting the atomic content on the surface or near the surface region of the nanoparticles [33]. Higher oxygen content (or lower iron content) was found in the sample with surfactant. This might be attributed to the oxygen from surfactant LAA that capped on the surface of magnetite nanoparticles [22,34].
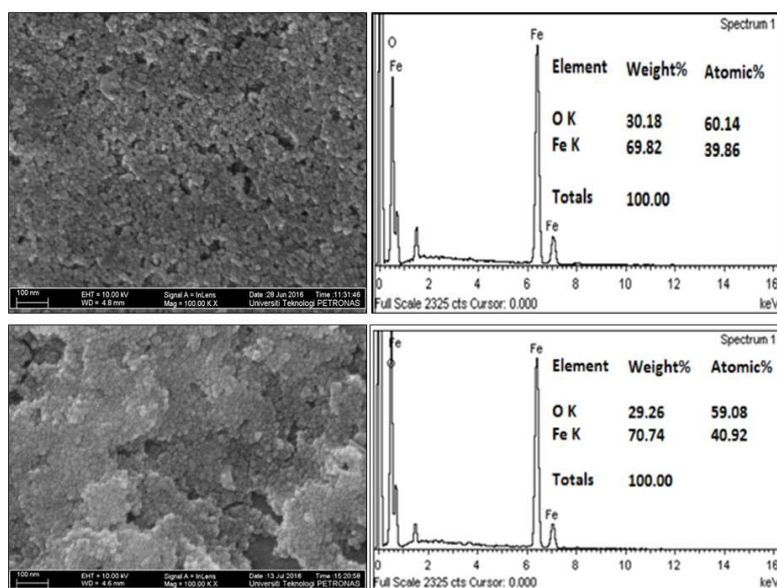
Fig. 2. SEM and EDX of samples synthesized with (a,b) LAA (FE2A0.96) and (c,d) without surfactant (FE20)

Transmission electron microscopy analysis was carried out to give a better illustration and understanding of the size distribution of the synthesized nanoparticles. Figure 3a and 3b presented the TEM image and particle size distribution of magnetite nanoparticles without LAA coating, whereas figure 3c and 3d showed the TEM image and particle size distribution of magnetite nanoparticles which synthesized with 0.96g of LAA. In general, spherical shape of nanoparticles were observed in both TEM images (figure 3a and 3c), which in a good agreement with the result of SEM images. From figure 3a and 3b, the magnetite nanoparticles had average particle size of 12.6 nm and the nanoparticles were agglomerated in cluster form. The attractive magnetic force and the high surface area over volume ratio of the magnetite nanoparticles cause the nanoparticles possessed high surface energies and consequently tend to agglomerate into cluster form in order to minimize the surface energies [10]. In contrast, figure 3c and 3d showed the magnetite nanoparticles synthesized with the aid of LAA had average particle size of 11.1 nm and the magnetite nanoparticles were well separated and no agglomeration was noticed. A good correlation between the crystallite sizes and particle sizes obtained from Scherrer equation and TEM was further supports the crystalline structure of magnetite nanoparticles. Besides, it was observed that the magnetite nanoparticles synthesized with LAA having smaller particle size as compared to those magnetite nanoparticles synthesized without surfactant. This result is also in agreement with the Xiong's work in synthesized copper nanoparticles using LAA[19]. This was because oxidation products of LAA absorbed on the surface of magnetite nanoparticles and prevent the growth of nanoparticles, thus producing smaller particle size (will be discussed in detail in the possible mechanism part) as compare to those nanoparticles synthesized without surfactant [19].
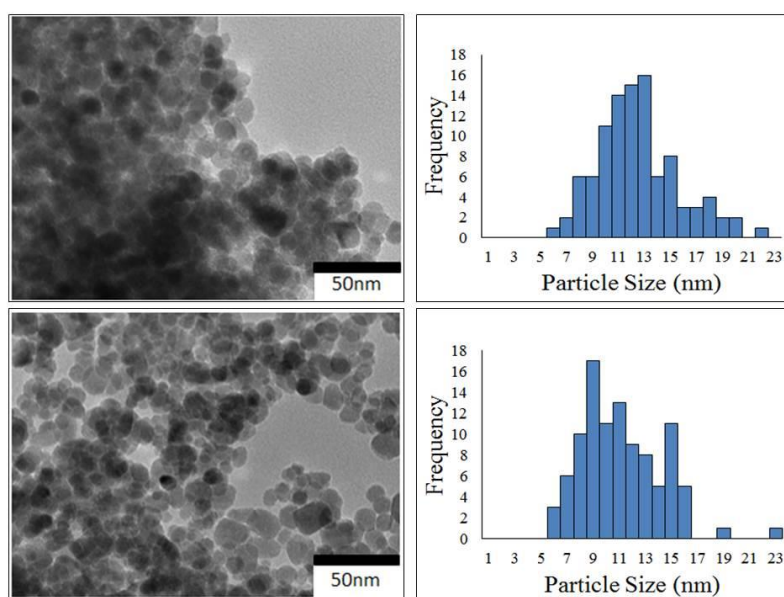
Fig. 3. TEM image and particle size distribution of samples (a-b) Magnetite nanoparticles without ascorbic acid (FE20) (c-d) with ascorbic acid FE2A0.96. The average particle size measured for samples without LAA and with LAA are 12.6 nm and 11.1 nm respectively

FTIR analysis was used to determine the possible functional group that attached on the surface of the synthesized nanoparticles [26]. Figure 4 shows the FTIR spectrum of the magnetite samples synthesized with different concentration of LAA. The pattern and number of peaks were similar and disregard to the concentration of LAA used in synthesizing magnetite nanoparticles. The only factor that affected by the changes of concentration of LAA was the intensity of the peaks. Magnetite nanoparticles synthesized with the addition of 0.96g of LAA had the most sharp and strongest intensity peaks as compared to others. Total of four obvious peaks at $572cm^{-1}$, $1400cm^{-1}$, $1672cm^{-1}$ and $3391cm^{-1}$ were observed. Peak at $572cm^{-1}$ is the characteristic of $M_{tetrahedral}$ resonance with O. This peak is related to the Fe-O stretching of Fe_3O_4 nanoparticles which confirm the formation of iron oxide nanoparticle [30, 35]. In this work, oxidation state of LAA ($C_6H_6O_6$) was capped with magnetite nanoparticles through carbonyl group. According to Tao and Am, there are two types of binding modes for surface carboxylate bonding [36]. The first mode is the carboxylate bound with the surface through oxygen atom, whereas the second mode is carboxylate bound symmetrically to the surface [37, 38]. The later mode occur in this work as the C=O stretching at $1400cm^{-1}$ [38]. In addition, C=O stretching at $1672cm^{-1}$ indicated the free carbonyl groups in $C_6H_6O_6$ [31]. Strong and broad peak at $3391cm^{-1}$ indicated the iron oxide surface covered with aqueous environment [39]. The presence of the hydroxyl groups on the surface of nanoparticles might be responsible for excellent dispersion of magnetite nanoparticles in aqueous environment which will be discussed in more detail at possible mechanism section [34]. Thus, from FTIR result, it is confirmed that the role of LAA as capping agent in synthesizing magnetite nanoparticles [19].
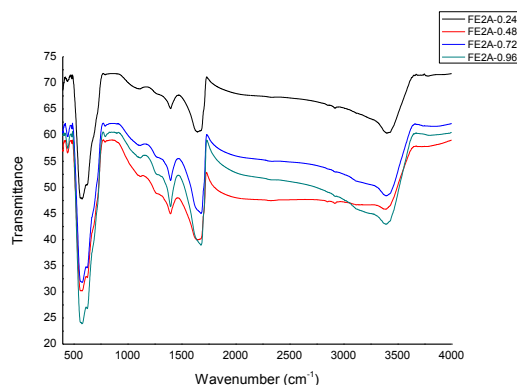
Fig. 4. FTIR for the magnetite samples synthesized with different concentration of LAA

The interaction between the magnetite nanoparticles and LAA is further investigated through XPS analysis. Figure 5 (a-c) shows the XPS spectra of magnetite nanoparticles synthesized at 80°C with and without LAA surfactant. In this case, XPS spectrum of magnetite nanoparticles without LAA acted as the reference. The C1s, O1s and Fe2p peaks as shown in figure 5a are located at 285eV, 532eV and 722eV, respectively, which proved the presence of both Fe_3O_4 and LAA [40]. It is observed that the XPS spectrum for the magnetite nanoparticles with LAA had a lower intensity and shows a shift to higher binding energy in all XPS spectra (whole range, Fe2p and O1 scan) as compare to reference peaks. The XPS spectra for Fe2p, peaks at 711.2eV, 719.4eV and 724.6eV were detected for reference peaks, but higher binding energy peaks (712.4eV, 721.2eV and 725.9eV) were shown for XPS spectra of magnetite nanoparticles coated with LAA. This may attributed to the binding effect from the LAA on the surface of magnetite nanoparticles [41]. From XPS spectrum of Fe2p that shown in figure 5b, total of two obvious peaks which located at 712.4eV and 725.9eV were noted. These two peaks are referred to $Fe2p^{3/2}$ in iron oxide and $Fe2p^{1/2}$ in LAA capped Fe_3O_4 nanoparticles and in good agreement with the literature value [42, 43]. Besides, the O1 peak as shown in figure 5c is located at 531.8eV again proved the presence of C=O of LAA capped on the surface of magnetite nanoparticles [40]. Therefore, the role of LAA is in accordance with previous result.
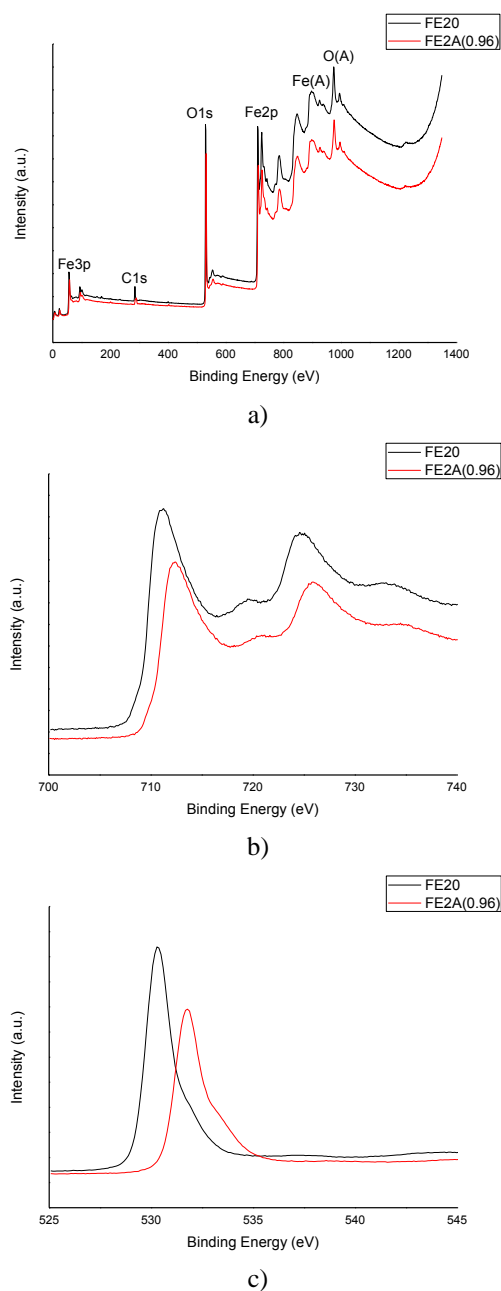
Fig. 5. XPS spectra of magnetite nanoparticles (a) in whole range (b) Fe2p and (c) O1s.

The stability of the nanoparticles dispersion was determined by the measurement of Zeta potential [44]. Magnetite nanoparticles synthesized with LAA produced stable particles suspension in DI water. Figure 6(a-d) presented the zeta potential for all cases (various concentration of LAA) was approximately -33mV, except for the magnetite nanoparticles synthesized with 0.96g of LAA had the Zeta potential value of -38mV. All the Zeta potential obtained for this samples series is fallen within the range of -33mv to -38mV which is considered to have high degree of stability [45]. The negative surface charge is expected due to the formation of dehydroascorbic acid which absorbed or capped on the surface of magnetite nanoparticles [44]. Dehydroascorbic acid had three carbonyl groups in its structure and thus contributes to high electronegativity [19]. The hydrolysis of dehydroascorbic acid formed polyhydroxyl group, which then form a complexion with magnetite nanoparticles by inter and intra hydrogen bonding, and eventually avoid aggregation

occurs [34]. As the capping effect of the oxidation products of LAA (refers to dehydroascorbic acid) increased the Zeta potential value of magnetite nanoparticles, the stability of the magnetite nanoparticles was increased due to the electrostatic repulsion among the negative charges [46]. The presence of LAA again proved its significant role in preventing the aggregation and production of smaller size of the magnetic nanoparticles [44].
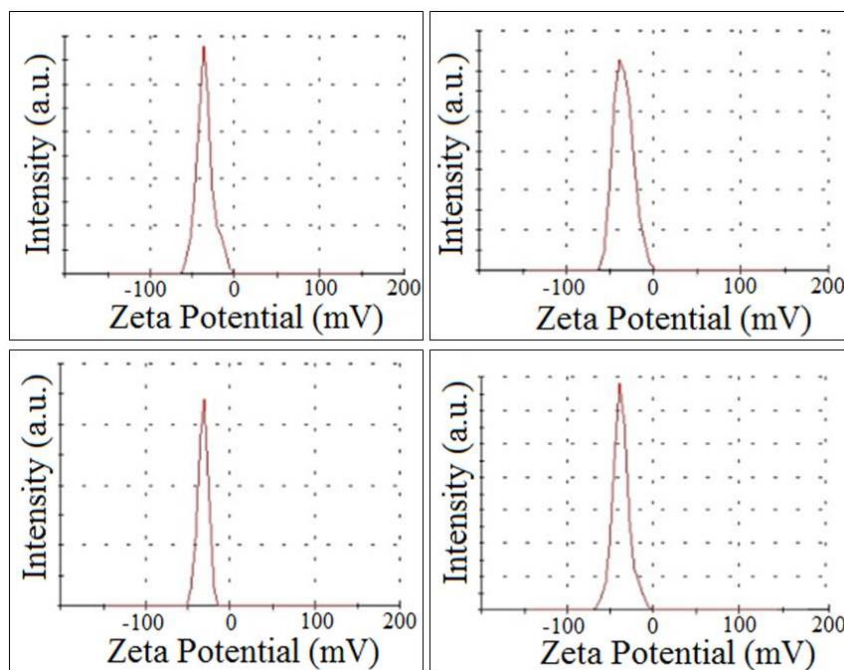

Fig. 6. Zeta potential of magnetite nanoparticles synthesized with various concentration of LAA, (a) FE2A0.24 (b) FE2A0.48 (c) FE2A0.72 and (d) FE2A0.96

VSM was used to carry out magnetic characterization of magnetite nanoparticles that synthesized at 80°C. Figure 7 shows the comparison of saturation magnetization of magnetite nanoparticles with and without LAA surfactant. The saturation magnetization value for magnetite nanoparticles that synthesized with 0.96g of LAA was 48.4 emu/g which was much smaller than 59.0 emu/g of magnetite nanoparticles that synthesized without LAA. The drop in the value of saturation magnetization is due to the presence of LAA surfactant on the surface of magnetite nanoparticles and also the smaller size of magnetite nanoparticles which eventually cause the reduction of magnetic moments of magnetite [47]. Smaller magnetite nanoparticles has large fraction for surface spins thus easily cause reduction of magnetic moments of magnetite as surface spin disorder that induced by reduce surface coordination and disjoin exchange bonds in the near surface layer [48]. In addition, the presence of LAA also contribute to the weight of the overall nanoparticles when it coated on the surface of magnetite nanoparticles, thus decrease the ratio of magnetite weight to overall weight, decrease the value of saturation magnetization [22]. The samples were exhibit superparamagnetic behavior as the coercivity of the synthesized magnetite nanoparticles was approximately 0 Oe as can be seen from figure 7 [49].
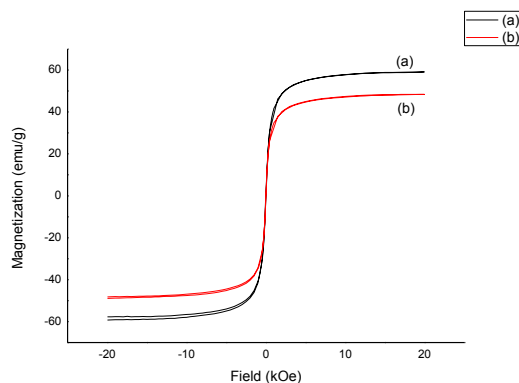
Fig. 7. VSM hysteresis loop of magnetite nanoparticles (a) without (FE20)

and (b) with LAA (FE2A0.96)

From the experimental results, a plausible mechanism on how LAA coated on magnetite nanoparticles was proposed. LAA is a highly water-soluble and strong polarity compound as it comprises of electrons from hydroxyl lone pair, double bond and lactone ring carbonyl double bond that can form conjugated system [19]. LAA mainly act as surfactant to prevent aggregation of nanoparticles whereas the ammonium hydroxide responsible to reduce Fe^{3+} to Fe^{2+} and consequently form more magnetite nanoparticles. The reaction in this study is presented in Equation (1).

$$FeSO_4.7H_2O + 2FeCl_3.6H_2O + 8NH_4OH \rightarrow$$
$$Fe_3O_4 + (NH_4)_2SO_4 + 6NH_4Cl + 17H_2O \qquad (1)$$
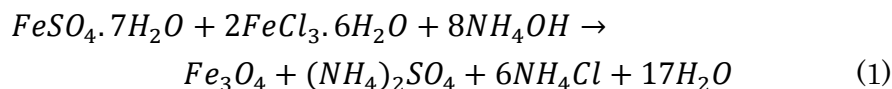
The stability of nanoparticles dispersion is the key factor in their application [34]. During the synthesis process, the lone pair electrons in the polar group of LAA reacted with magnetite nanoparticles through hydrogen bonding to form a complex compound as shown in figure 8. The LAA is thus capped with magnetite nanoparticles. Once the LAA has capped on the surface of nanoparticles, the stearic hindrance prevent the agglomeration and consequently decrease the particle size of magnetite nanoparticles [50].
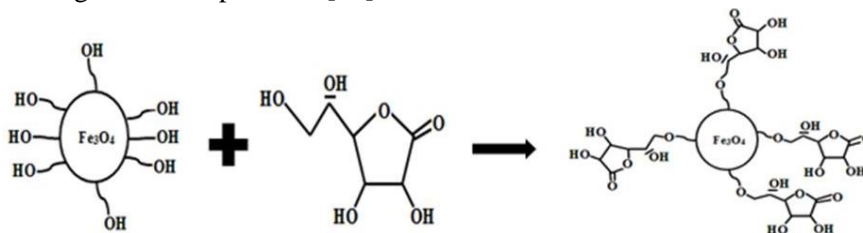

Fig. 8. Esterification of magnetite nanoparticle with LAA.

Another factor that contributes to the stability of magnetite nanoparticles is the dispersion effect of dehydroascorbic acid [19]. Dehydroascorbic acid is formed from LAA through the removal of two electrons and two protons through the oxidation process as illustrated in figure 9 [51].
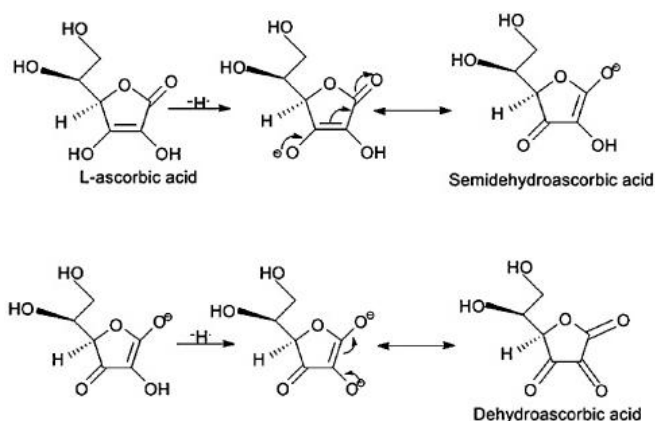
Fig. 9. Formation of dehydroascorbic acid from LAA [19].

The dehydroascorbic acid has three carbonyl groups which make it too electrophilic to stay in aqueous condition even just few milliseconds [34]. Thus, it quickly forms polyhydroxyl structure through hydrolysis as shown in figure 10 [52].
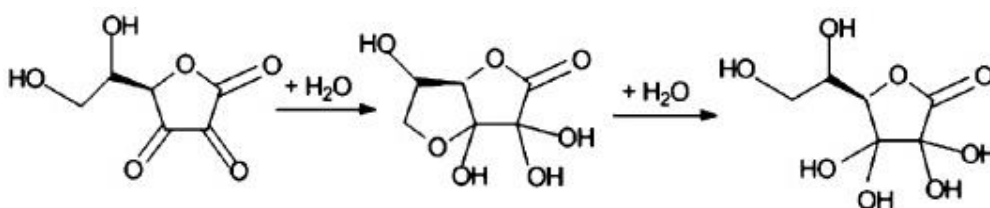

Fig. 10. Hydrolysis of dehydroascorbic acid [52].

The presence of many hydroxyl groups can facilitate the formation of complex magnetite nanoparticles by inter and intramolecular hydrogen bonding and thus avoid the aggregation occurs [19,34].

4. Conclusions

In conclusion, magnetite nanoparticles with the addition of various concentration of LAA were synthesized through an eco-friendly approach. 0.96g of LAA used for synthesizing magnetite nanoparticles provide the best result as compare to the other concentrations that were employed. LAA served as capping agent and stabilizer in the synthesis process. Smaller particle size, no aggregation and high stability dispersion of magnetite nanoparticles were produced. The synthesized magnetite nanoparticles exhibit superparamagnetic behavior. Thus, this modified method is a simple, cost-effective and more environmental friendly approach to produce magnetite nanoparticles. From the results obtained, the LAA coated magnetite nanoparticles are expected to present some biomedical applications.

References

[1]J. Peng, Q. Liu, Z. Xu, J. Masliyah,Energy Fuels**26**, 2705 (2012).

[2]G. Liu, X. Xu, J. Gao,Energy Fuels**17**, 543 (2003).

[3]J. Liang, H. Li, J. Yan, W. Hou, Energy Fuels**28**, 6172 (2014).

[4]S. Li, N. Li, S. Yang, F. Liu, J. Zhou,J. Mater. Chem. A**2**, 94 (2014).

[5]H. Maruyama, H.Seki, Y. Satoh,Water Res.**46**, 3094 (2012).

[6]J. S. Eow, M. Ghadiri, Chem. Eng.**85**, 357 (2002).

[7]R. Martínez-Palou,R. Cerón-Camacho, B. Chávez,A. A. Vallejo, D. Villanueva-Negrete, J. Castellanos, J. Aburto,Fuel**113**, 407 (2013).

[8]N. Ali, B. Zhang, H. Zhang, W. Zaman, X. Li, W. Li, Q. Zhang,Colloids Surf. A.Physicochem. Eng. Asp.**472**, 38 (2015).

[9] J. Liang, N. Du, S. Song, W. Hou,Colloids Surf. A Physicochem. Eng. Asp.**466**,197(2015).

[10] M. Senthil, C. Ramesh,Dig. J. Nanomater. Biostruct. **7**, 1655 (2012).

[11] M. Mahdavi, F. Namvar, M. B. Ahmad, R. Mohamad, Molecules **18**, 5954 (2013).

[12] M. Babincova, P. Sourivong, D. Leszczynska, P. Babinec,Med. Hypotheses **55**,459 (2000).

[13] J. Liu, Z. Sun, Y. Deng, Y. Zou, C. Li, X. Guo, D. Zhao,Angew. Chem.**121**, 5989 (2009).

[14] A. H. Lu, E. E. Salabas, F. Schüth, Angew. Chem. Int. Ed. **46**, 1222(2007).

[15] J. Peng, Q. Liu, Z. Xu, J. Masliyah, Adv. Funct. Mater.**22**, 1732(2012).

[16] A. M. Awwad, B. A. Albiss,N. M. Salem,J. Sikkim Manipal University (SMU) Med. **2**, 91(2015).

[17] M. J. Ahmed, J. Bioprocess. Chem. Eng.**2**, 1 (2014).

[18] S. L. Y. Tang, R. L. Smith, M.Poliakoff, Green Chem.**7**,761 (2005).

[19] J. Xiong, Y. Wang, Q. Xue, X. Wu,Green Chem.**13**, 900 (2011).

[20] W. Wu, Q. He, C. Jiang,Nanoscale Res. Lett.**3**, 397(2008).

[21] V. Sreeja, K. N. Jayaprabha, P. A. Joy, Appl.Nanosci.**5**, 435 (2015).

[22] N. Neyaz, M. S. S. Zarger,W. A. Siddiqui,Int. J. Environ. Sci. **5**,260 (2014).

[23] M. W. Davey, M. V. Montagu, D.Inze, M. Sanmartin, A. Kanellis, N. Smirnoff, I.J. Benzie, J. J. Strain, D. Favell,J. Fletcher,J. Sci. Food Agr. **80**, 825 (2000).

[24] J. Zhang, H. Yang, G. Shen, P. Cheng, J. Zhang,S. Guo,Chem. Commun. **46**,1112(2010).

[25] S. Smaoui, H. B. Hlima, A. Kadri,J. Chem. Soc. Pak. **35**, 1096 (2013).

[26] I. H. Ibrahim, S. M.Sallam, H. Omar, M. Rizk, Int. J. Biomed. Sci. **2**, 295(2006).

[27] L. Feng, M. Cao, X. Ma, Y. Zhu, C.Hu, J. Hazard. Mater.**217**, 439 (2012).

[28] G. L. Li, Y. R. Jiang, K. L. Huang, P. Ding,I. I. Yao, J. Colloid Interface Sci.**320**, 11(2008).

[29] F. Ozel, H. Kockar, O. Karaagac,J. Supercond. Nov. Magn.**28**, 823 (2015).

[30] N. D. Kandpal, N. Sah, R. Loshali, R. Joshi, J. Prasad, J. Sci. Ind. Res. **73**, 87(2014).

[31] S. Xuan, L. Hao, W. Jiang, X. Gong, Y. Hu, Z. Chen, J. Magn. Magn. Mater. **308**, 210(2007).

[32] M. M. Rahman,Nanomaterials, European Union: Intech Publisher,Croatia (2011).

[33] M. Balamurugan, S. Saravanan, T. Soga,E-j. Surf. Sci. Nanotechnol. **12**, 363 (2014).

[34] S. Jain, A. Jain, P. Kachhawah, V. Derva, Trans. Nonferrous Met. Soc. China**25**, 3995(2015).

[35] M.G. Balamurughan, S. Mohanraj, S. Kodhaiyolii, V. Pugalenthi, J. Chem. Pharm. Sci. **1**, 201 (2014).

[36] Y. T. Tao, J. Am. Chem. Soc.**115**, 4350 (1993).

[37] K. V. Shafi, A. Ulman, X. Z. Yan, N. Yang, C. Estournes, H. White, M. Rafailovich, J. Am.

Chem. Soc. **17**, 5093(2001).

[38] L. A. Harris, J. D. Goff, A. Y. Carmichael, J. S. Riffle, J. J. Harburn, T. G. St. Pierre, M. Saunders,Chem. Mater. **15**, 1367 (2003).

[39] F. Y. Cheng, C. H. Su, Y. S. Yang, C. S. Yeh, C. Y. Tsai, C. L. Wu, M. T. Wu, D. B. Shieh, Biomaterials **26**,729 (2005).

[40] Y. Zhang, J. Y. Liu, S. Ma, Y. J. Zhang, X. Zhao, X. D. Zhang, Z. D. Zhang, J. Mater. Sci. Mater. Med. **21**, 1205(2010).

[41] S. Mohapatraa, P. Pramanik,Colloids Surf. A Physicochem. Eng. Asp. **339**, 35(2009).

[42] E. Paparazzo, Appl. Surf. Sci. **25**, 1(1986).

[43] T. Shahwan, S. A. Sirriah, M. Nairat, E.Boyaci, A. E. Eroglu, T. B. Scott,K. R. Hallam, Chem. Eng.**172**, 258 (2011).

[44] W. W. Drzewiecka, S. Gaikwad, D. Laskowski, H. Dahm, J. Niedojadlo, A. Gade, M. Rai, Austin J. Biotechnol. Bioeng.**1**, 1 (2014).

[45] Zeta Potential Analysis of Nanoparticles NanoComposix, San Diego, CA (2012).

[46] S. Kalliola, E. Repo, M. Sillanpää, J. S. Arora, J. He,V. T. John,Colloids Surf. A Physicochem. Eng. Asp.**493**, 99(2016).

[47] S. Koesnarpadi, S. J.Santosa, D.Siswanta,B. Rusdiarso,Procedia Environ. Sci. **30**, 103(2015).

[48] R. P. Araújo-Neto, E. L. Silva-Freitas, J. F. Carvalho, T. R. F., Pontes, K. L. Silva, I. H. M. Damasceno, E. S.T. Egito, A. Dantas, M. Morales, A. Carriço, J.Magn. Magn. Mater.**364**, 72(2014).

[49] S. Kekutia, L. Saneblidze, V. Mikelashvili, J. Markhulia, R. Tatarashvili, D. Daraselia, D. Japaridze, Eur. Chem. Bull.**4**,33 (2015).

[50] D. Rehana, A. K. Haleel, A. K. Rahiman, J. Chem. Sci. **127**, 1155 (2015).

[51] M. A. Farrukh, M. Saud, N. Siraj,I. I. Naqvi,The Nucleus **40**,91(2003).

[52] E. Kimoto, H. Tanaka, T. Ohmoto, M. Choami,Anal. Biochem. **214**, 38 (1993).